AMERICAN SOCIETY FOR MICROBIOLOGY | Microbiology Spectrum

OBSERVATION

Broad-Spectrum *In Vitro* Antiviral Activity of ODBG-P-RVn: An Orally-Available, Lipid-Modified Monophosphate Prodrug of Remdesivir Parent Nucleoside (GS-441524)

Michael K. Lo,[a] Punya Shrivastava-Ranjan,[a] Payel Chatterjee,[a] Mike Flint,[a] James R. Beadle,[b] Nadejda Valiaeva,[b] Joyce Murphy,[b] Robert T. Schooley,[b] Karl Y. Hostetler,[b] Joel M. Montgomery,[a] Christina F. Spiropoulou[a]

[a]Viral Special Pathogens Branch, Centers for Disease Control and Prevention, Department of Health and Human Services, Atlanta, Georgia, USA
[b]Division of Infectious Diseases and Global Public Health, Department of Medicine, University of California San Diego, La Jolla, California, USA

ABSTRACT The necessity for intravenous administration of remdesivir confines its utility for treatment of coronavirus disease 2019 (COVID-19) to hospitalized patients. We evaluated the broad-spectrum antiviral activity of ODBG-P-RVn, an orally available, lipid-modified monophosphate prodrug of the remdesivir parent nucleoside (GS-441524), against viruses that cause diseases of human public health concern, including severe acute respiratory syndrome coronavirus 2 (SARS-CoV-2). ODBG-P-RVn showed 20-fold greater antiviral activity than GS-441524 and had activity nearly equivalent to that of remdesivir in primary-like human small airway epithelial cells. Our results warrant *in vivo* efficacy evaluation of ODBG-P-RVn.

IMPORTANCE While remdesivir remains one of the few drugs approved by the FDA to treat coronavirus disease 2019 (COVID-19), its intravenous route of administration limits its use to hospital settings. Optimizing the stability and absorption of remdesivir may lead to a more accessible and clinically potent therapeutic. Here, we describe an orally available lipid-modified version of remdesivir with activity nearly equivalent to that of remdesivir against emerging viruses that cause significant disease, including Ebola and Nipah viruses. Our work highlights the importance of such modifications to optimize drug delivery to relevant and appropriate human tissues that are most affected by such diseases.

KEYWORDS SARS-CoV-2, Ebola virus, Nipah virus, respiratory viruses, hemorrhagic fever virus, filovirus, paramyxovirus, henipavirus, remdesivir, GS-5734, remdesivir nucleoside, GS-441524, antiviral agents, lipid prodrugs, ODBG, Vero E6 cells, Huh7 cells, NCI-H358 cells, human telomerase reverse-transcriptase (hTERT)-immortalized microvascular endothelial cells (TIME), human small airway epithelial cells, HSAEC1-KT, ODBG-P-RVn

Remdesivir (RDV; Veklury, GS-5734) is an adenosine nucleotide analog phosphoramidate prodrug with broad-spectrum antiviral activity *in vitro* and *in vivo* (1) and is currently the only FDA-approved therapeutic for treating coronavirus 2019 disease (COVID-19) in hospitalized patients over the age of 12 (2). While RDV did not significantly reduce COVID-19 mortality, it shortened the time to recovery compared to the time for placebo controls (3). The short half-life of RDV in human and animal plasma (4–7), alongside the *in vivo* efficacy of the RDV parent nucleoside (RVn; GS-441524) against coronaviruses, including severe acute respiratory syndrome coronavirus 2 (SARS-CoV-2) (8–11), have driven proposals to utilize the RVn instead of RDV to treat COVID-19 (12). A recent comparative pharmacokinetic study in nonhuman primates, however, demonstrated higher levels of the active metabolite RVn-triphosphate (RVn-TP) in lower respiratory tract tissues of RDV-dosed animals than in RVn-dosed animals

Editor Manjula Kalia, Regional Centre for Biotechnology

This is a work of the U.S. Government and is not subject to copyright protection in the United States. Foreign copyrights may apply.

Address correspondence to Michael K. Lo, mko2@cdc.gov, or Christina F. Spiropoulou, ccs8@cdc.gov.

Received 12 October 2021
Accepted 28 October 2021
Published 24 November 2021

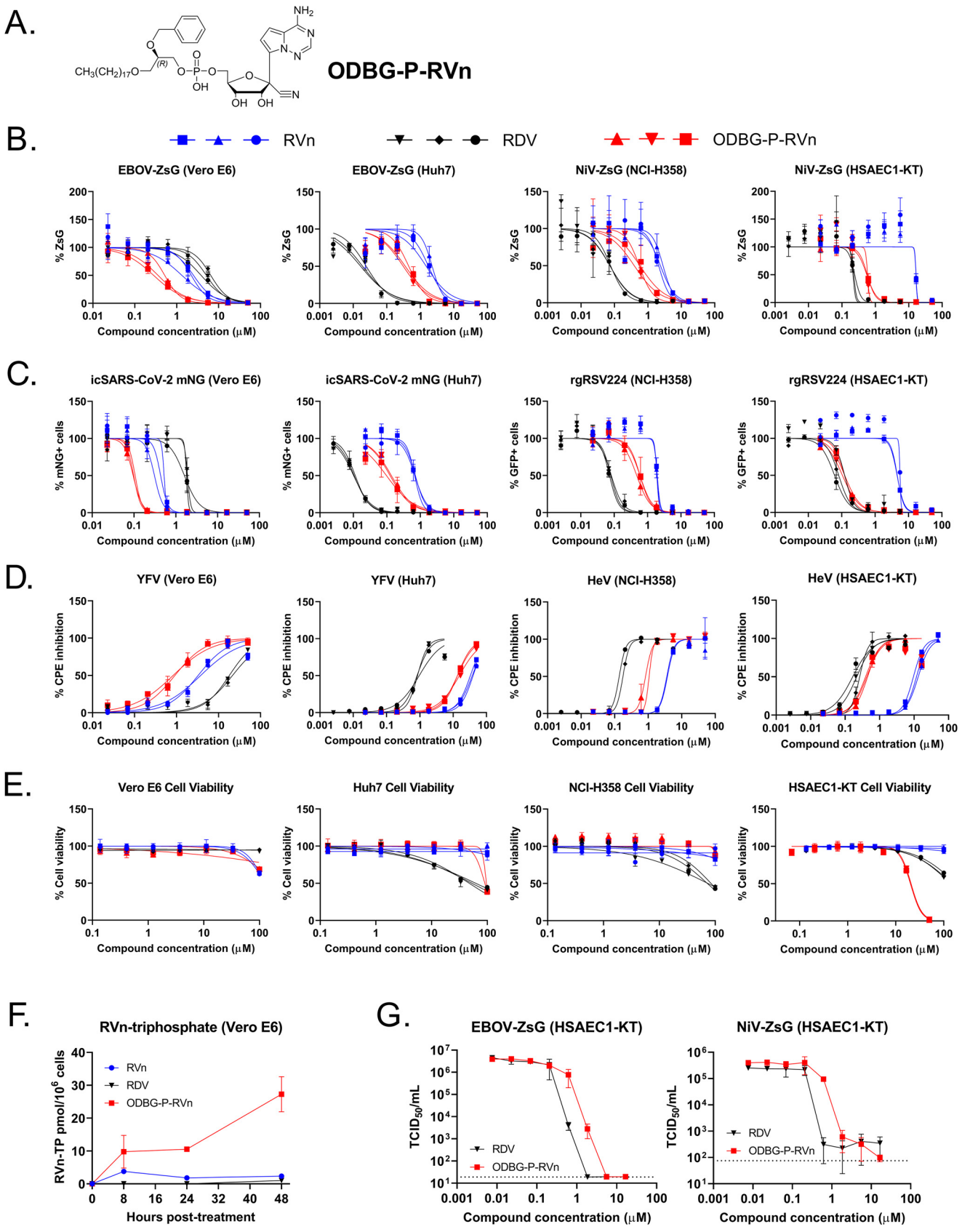

FIG 1 Comparison of antiviral activities of RVn, RDV, and ODBG-P-RVn in African green monkey (Vero-E6), human hepatoma (Huh7), human bronchioalveolar carcinoma (NCI-H358), and primary-like human telomerase reverse transcriptase-immortalized small airway epithelial (HSAEC1-KT) cell

(Continued on next page)

(6). A significant drawback of RDV is the requirement for intravenous administration, which limits its use to hospital contexts. To develop an orally bioavailable form of remdesivir, we recently synthesized a 1-*O*-octadecyl-2-*O*-benzyl-*sn*-glycerylester (ODBG) lipid-modified monophosphate prodrug of RVn (ODBG-P-RVn) ($C_{40}H_{62}N_5O_9P$) (Fig. 1A), which demonstrated more favorable *in vitro* antiviral activity than RVn and RDV against SARS-CoV-2 in Vero-E6 cells (13).

In this study, we extended our *in vitro* comparisons to include 14 viruses from 7 virus families responsible for causing diseases of significant human public health concern. These were Ebola virus (EBOV) and Marburg virus (MARV) from the family *Filoviridae*, Nipah virus (NiV), Hendra virus (HeV), human parainfluenza virus 3 (hPIV3), measles virus (MV), mumps virus (MuV), and Sosuga virus (SoSuV) from the family *Paramyxoviridae*, respiratory syncytial virus (RSV) from the family *Pneumoviridae*, yellow fever virus (YFV) from the family *Flaviviridae*, Lassa virus (LASV) from the family *Arenaviridae*, Crimean-Congo hemorrhagic fever virus (CCHFV) from the family *Nairoviridae*, and SARS-CoV-2 from the family *Coronaviridae* (14–18). We utilized the following three previously described assays to compare the antiviral activities of RVn, RDV, and ODBG-P-RVn against this panel of viruses (15, 17): (i) directly measuring the fluorescence of a reporter protein expressed by recombinant viruses (REP) (Fig. 1B), (ii) quantitating focus-forming units (FFU) via fluorescent-reporter imaging (Fig. 1C), and (iii) indirectly measuring cytopathic effect (CPE) based on cellular ATP levels (CellTiterGlo 2.0; Promega) (Fig. 1D), which was also used to evaluate compound cytotoxicity (Fig. 1E). Assay conditions varied based on virus replication kinetics and on the specific assay used; the multiplicities of infection (MOIs) ranged from 0.01 to 0.25, and endpoint measurements were conducted between 72 and 144 h postinfection (hpi) (see Methods in the supplemental material). We conducted dose-response experiments using 8-point, 3-fold serial dilutions of RVn, RDV, and ODBG-P-RVn against our panel of viruses in Vero-E6 cells and showed that ODBG-P-RVn consistently had greater antiviral activity than RVn and RDV against all viruses susceptible to RVn/RDV inhibition, with 50% effective concentration (EC_{50}) values ranging from 0.026 to 1.13 μM (Fig. 1B to D, left; Table 1; Fig. S1 in the supplemental material). RVn and ODBG-P-RVn induced partial cytotoxicity but only at the highest concentration tested (100 μM) and without reaching 50% cytotoxic concentration (CC_{50}). To understand the comparatively greater potency of ODBG-P-RVn in Vero E6 cells, we measured the levels of RVn-TP in cells treated with RVn, RDV, or ODBG-P-RVn. We observed that RVn-TP levels indeed correlated with antiviral activity, with ODBG-P-RVn consistently accumulating to higher levels than both RVn and RDV across 3 time points (Fig. 1F). We then compared these antivirals in human hepatoma (Huh7) and bronchioalveolar carcinoma (NCI-H358) cell lines, which represent more-relevant cell types that are targeted by subsets of viruses used in our study. In both human cell lines, although ODBG-P-RVn showed EC_{50} values comparable to those observed in Vero-E6 cells and was 3- to 5-fold

FIG 1 Legend (Continued)
lines using fluorescent-reporter-based, image-based, and cytopathic effect (CPE) assays. Values for representative dose-response inhibition of viral replication and induction of cellular cytotoxicity by RVn, RDV, and ODBG-P-RVn are shown. (A) The chemical structure of ODBG-P-RVn. (B) Direct measurement of reporter fluorescence intensities from recombinant Ebola virus (EBOV) expressing ZsGreen protein in Vero-E6 (left) and Huh7 (middle left) cells and recombinant Nipah virus (NiV) expressing ZsGreen protein in NCI-H358 (middle right) and HSAEC1-KT (right) cells. (C) Image-based counting of reporter fluorescence-positive cells infected with recombinant severe acute respiratory syndrome coronavirus 2 (SARS-CoV-2) expressing mNeonGreen protein (Vero-E6 and Huh7 cells) and recombinant respiratory syncytial virus (RSV) expressing enhanced green fluorescent protein (eGFP) (NCI-H358 and HSAEC1-KT cells). Values for infected cells treated with dimethyl sulfoxide (DMSO) were considered the 100% fluorescence intensity signals and 100% fluorescence-positive cell counts. (D) Compound-based inhibition of CPE induced by yellow fever virus (YFV) (Vero-E6 and Huh7 cells) and by Hendra virus (HeV) (NCI-H358 and HSAEC1-KT cells) determined by measuring cellular ATP levels (CellTiterGlo 2.0). ATP levels in uninfected cells treated with DMSO were considered 100% CPE inhibition. (E) Compound cytotoxicity/cell viability for the respective cell lines used measured by CellTiterGlo 2.0 assay. (F) Measurement of RVn-triphosphate (RVn-TP) levels in Vero E6 cells treated with RVn, RDV, or ODBG-P-RVn at various time points until 48 h posttreatment. (G) Reductions of infectious yields of EBOV-ZsG (left) and NiV-ZsG (right) by RDV and ODBG-P-RVn in HSAEC1-KT cells. *y* axis denotes 50% tissue culture infectious dose ($TCID_{50}$) expressed in logarithmic scale. Dose-response curves for antiviral assays in panels B, C, and D were fitted to the mean values of experiments performed in biological triplicate for each concentration in the 8-point, 3-fold dilution series using a 4-parameter nonlinear logistic regression curve with variable slope. Data points and error bars indicate the mean values and standard deviations from 3 biological replicates; each colored shape/line in the legend represents an independent experiment performed in biological triplicate as indicated above panel B. Infectious yield reduction assays were conducted once in biological quadruplicates. RVn and RDV used in this study were obtained from MedChemExpress (Monmouth Junction, NJ, USA).

TABLE 1 Mean antiviral activities of RVn, RDV, and ODBG-P-RVn in Vero E6, Huh7, and NCI-H358 cell lines

			Mean value (μM) ± SD for indicated antiviral in indicated cells[d]																
			Vero E6									Huh7/NCI-H358[e]							
			RVn (GS-441524)			RDV (GS-5734)			ODBG-P-RVn			RVn (GS-441524)			RDV (GS-5734)			ODBG-P-RVn		
Virus family	Virus[a]	Species/variant[b]	Assay[c]	EC_{50}	EC_{90}	SI (CC_{50} > 100 μM)	EC_{50}	EC_{90}	SI (CC_{50} > 100 μM)	EC_{50}	EC_{90}	SI (CC_{50} > 100 μM)	EC_{50}	EC_{90}	SI (CC_{50} > 100 μM/ >100)	EC_{50}	EC_{90}	SI (CC_{50}: 54.2 ± 6.0/ 77.2 ± 5.3)	EC_{50}	EC_{90}	SI (CC_{50}: 93.4 ± 3.0/ >100)
Filoviridae	EBOV	Rec. Makona-ZsG	REP	2.03 ± 0.50	7.54 ± 1.09	49	5.15 ± 1.09	17.31 ± 0.89	>19	0.39 ± 0.10	1.71 ± 0.25	>258	**1.84 ± 0.31**	**6.91 ± 1.79**	**>54**	**0.020 ± 0.003**	**0.16 ± 0.02**	**2,710**	**0.37 ± 0.06**	**2.13 ± 0.37**	**251**
	MARV	Rec. Bat371-ZsG	REP	0.96 ± 0.09	4.05 ± 1.42	104	2.16 ± 0.27	10.22 ± 2.02	>46	0.19 ± 0.04	0.81 ± 0.12	>521	**1.92 ± 0.06**	**4.47 ± 0.48**	**>52**	**0.025 ± 0.002**	**0.075 ± 0.003**	**2,128**	**0.33 ± 0.02**	**0.99 ± 0.09**	**285**
Paramyxoviridae	NiV-M	Rec. Malaysia-ZsG	REP	1.10 ± 0.40	2.20 ± 1.05	73	5.87 ± 0.19	9.82 ± 0.43	>16	0.31 ± 0.04	0.78 ± 0.28	>196	2.43 ± 0.31	5.95 ± 1.10	>41	0.075 ± 0.001	0.31 ± 0.04	1,026	0.50 ± 0.06	2.83 ± 1.39	>198
			CPE	0.48 ± 0.06	0.78 ± 0.19	207	3.34 ± 0.34	5.39 ± 0.29	>30	0.19 ± 0.01	0.30 ± 0.04	>522	ND	ND	NA	ND	ND	NA	ND	ND	NA
	NiV-B	Bangladesh	CPE	0.52 ± 0.02	1.14 ± 0.02	192	2.84 ± 0.10	5.81 ± 0.44	>35	0.17 ± 0.01	0.38 ± 0.04	>599	3.42 ± 0.005	5.41 ± 0.29	>29	0.12 ± 0.0004	0.19 ± 0.01	661	0.82 ± 0.053	1.38 ± 0.05	>122
	HeV	1996	CPE	1.43 ± 0.17	12.06 ± 3.14	70	4.56 ± 0.20	17.58 ± 3.91	>22	0.37 ± 0.04	3.93 ± 1.98	>270	3.68 ± 0.08	6.33 ± 0.18	>27	0.16 ± 0.02	0.25 ± 0.03	491	0.95 ± 0.12	1.42 ± 0.03	>105
	MV	Rec. rMV^{EZ}GFP(3)	REP	0.58 ± 0.20	1.71 ± 0.07	172	4.97 ± 0.25	6.12 ± 0.3	>20	0.16 ± 0.03	0.21 ± 0.01	>609	0.88 ± 0.16	6.99 ± 1.90	>113	0.025 ± 0.007	0.13 ± 0.09	3,074	0.12 ± 0.003	0.86 ± 0.22	>803
	hPIV3	Rec. JS-GFP	FFU	0.14 ± 0.01	0.28 ± 0.02	70	0.43 ± 0.09	0.90 ± 0.03	>232	0.026 ± 0.002	0.050 ± 0.002	>3,896	1.43 ± 0.16	1.98 ± 0.05	>70	0.031 ± 0.002	0.052 ± 0.01	2,458	0.22 ± 0.01	0.43 ± 0.02	>457
	MuV	Rec. IA2006-eGFP	FFU	5.11 ± 0.20	7.80 ± 0.64	18	16.81 ± 1.23	25.1 ± 1.97	>4.9	1.13 ± 0.04	2.53 ± 0.25	>56	**9.3 ± 0.30**	**13.71 ± 0.24**	**>11**	**0.20 ± 0.003**	**0.24 ± 0.003**	**266**	**1.85 ± 0.11**	**2.24 ± 0.23**	**50**
	SoSuV	Rec. 2012-ZsG	REP	1.00 ± 0.10	2.72 ± 0.62	100	5.31 ± 1.8	19.10 ± 9.31	>19	0.31 ± 0.089	0.80 ± 0.06	>325	**2.06 ± 0.09**	**7.76 ± 1.11**	**>48**	**0.052 ± 0.01**	**0.13 ± 0.02**	**1,042**	**0.52 ± 0.10**	**1.08 ± 0.15**	**180**
Pneumoviridae	RSV	Rec. rgRSV0224 (A2)	FFU	0.49 ± 0.05	0.62 ± 0.01	206	1.80 ± 0.08	2.40 ± 0.27	>55	0.10 ± 0.02	0.22 ± 0.03	>997	1.93 ± 0.02	2.36 ± 0.08	>51	0.078 ± 0.004	0.17 ± 0.02	991	0.55 ± 0.057	1.41 ± 0.09	>180
Coronaviridae	SARS-CoV-2	Rec. icSARS-CoV-2 mNG (WA1)	FFU	0.42 ± 0.09	0.60 ± 0.06	236	1.77 ± 0.13	2.81 ± 0.78	>56	0.10 ± 0.005	0.16 ± 0.01	>997	**0.69 ± 0.01**	**1.50 ± 0.20**	**>144**	**0.011 ± 0.001**	**0.035 ± 0.002**	**5,073**	**0.12 ± 0.02**	**0.69 ± 0.07**	**778**
Flaviviridae	YFV	17D	CPE	3.52 ± 0.24	30.25 ± 10.08	28	19.86 ± 1.73	>50	>5	0.87 ± 0.043	7.37 ± 1.59	>114	**36.83 ± 2.85**	**>50**	**>2.7**	**0.88 ± 0.057**	**3.09 ± 1.47**	**62**	**14.11 ± 0.90**	**>50**	**6.6**
Arenaviridae	LASV	Rec. Josiah-ZsG	REP	NI	NI	NA	NI	NI	NA	31.14 ± 7.79	>50	>3	**NI**	**NI**	**NA**	**2.87 ± 0.61**	**5.17 ± 0.33**	**19**	**NI**	**NI**	**NA**
Nairoviridae	CCHFV	Rec. IbAr10200-ZsG	REP	NI	NI	NA	NI	NI	NA	NI	NI	NA	**NI**	**NI**	**NA**	**NI**	**NI**	**NA**	**NI**	**NI**	**NA**

[a]EBOV, Ebola virus; MARV, Marburg virus; NiV-M, Nipah virus Malaysia strain; NiV-B, Nipah virus Bangladesh strain; HeV, Hendra virus; MV, measles virus; hPIV3, human parainfluenza virus 3; MuV, mumps virus; SoSuV, Sosuga virus; RSV, respiratory syncytial virus; SARS-CoV-2, severe acute respiratory syndrome coronavirus 2; YFV, yellow fever virus; LASV, Lassa virus; CCHFV, Crimean-Congo hemorrhagic fever virus.

[b]Rec., recombinant; ZsG, ZsGreen fluorescent protein; GFP, green fluorescent protein; eGFP, enhanced GFP; mNG, mNeonGreen.

[c]REP, CPE, and FFU assays were conducted between 72 and 144 hpi. REP, fluorescent reporter; CPE, cytopathic effect; FFU, focus-forming units.

[d]Values were derived from 3 independent experiments performed in biological triplicates, except for assays of NiV-B (NCI-H358 cells), HeV (NCI-H358 cells), and YFV (Vero E6 cells), which were performed twice in biological triplicates. EC_{50}, EC_{90}, and CC_{50} values were calculated using GraphPad Prism 9 software. EC_{50} and EC_{90}, 50% and 90% effective concentrations; CC_{50}, 50% cytotoxic concentration; SI, selective index (EC_{50}/CC_{50}); ND, not determined; NI, no inhibition; NA, not applicable. The CC_{50} values for each compound in the respective cell lines are indicated in parentheses above the column indicated for SI values.

[e]Data in boldface were derived from Huh7 cells, and underlined data were derived from NCI-H358 cells.

TABLE 2 Mean antiviral activities of RVn, RDV, and ODBG-P-RVn in TIME and HSAEC1-KT cell lines

				Mean value (μM) ± SD for indicated antiviral in indicated cells[d]																
				HSAEC1-KT									TIME							
				RVn (GS-441524)			RDV (GS-5734)			ODBG-P-RVn			RVn (GS-441524)			RDV (GS-5734)			ODBG-P-RVn		
Virus family	Virus[a]	Species/variant[b]	Assay[c]	EC_{50}	EC_{90}	SI (CC_{50} > 100 μM)	EC_{50}	EC_{90}	SI (CC_{50} > 100 μM)	EC_{50}	EC_{90}	SI (CC_{50} = 20.5 ± 0.29 μM)	EC_{50}	EC_{90}	SI (CC_{50} > 100 μM)	EC_{50}	EC_{90}	SI (CC_{50} = 17.2 ± 0.42 μM)	EC_{50}	EC_{90}	SI (CC_{50} > 50 μM)
Filoviridae	EBOV	Rec. Makona-ZsG	REP	10.7 ± 2.62	21.79 ± 3.16	>9.3	0.17 ± 0.02	0.41 ± 0.14	>587	0.21 ± 0.02	1.06 ± 0.18	98	14.88 ± 0.28	17.24 ± 0.16	>3.36	0.13 ± 0.04	0.2 ± 0.01	132	0.99 ± 0.063	1.96 ± 0.043	>50
			VTR	ND	ND	NA	0.11	0.82	>909	0.21	0.95	98	ND	ND	NA	0.032	0.064	530	0.15	0.39	>324
	MARV	Rec. Bat371-ZsG	REP/FFU	35.53 ± 7.07	71.35 ± 1.28	>2.8	0.75 ± 0.19	2.92 ± 0.14	>133	0.71 ± 0.11	3.67 ± 0.49	29	5.2 ± 0.26	6.89 ± 0.86	>9.61	0.04 ± 0.003	0.086 ± 0.004	430	0.23 ± 0.036	0.66 ± 0.032	>213
Paramyxoviridae	NiV-M	Rec. Malaysia-ZsG	REP	16.46 ± 0.04	19.12 ± 0.05	>6.1	0.23 ± 0.01	0.31 ± 0.06	>440	0.57 ± 0.013	0.97 ± 0.21	36	13.53 ± 2.44	17.52 ± 0.77	>3.70	0.10 ± 0.01	0.20 ± 0.01	172	0.75 ± 0.05	2.01 ± 0.30	>66
			CPE	16.12 ± 4.21	78.1 ± 35.08	>6.2	0.31 ± 0.04	0.075 ± 0.004	>318	0.90 ± 0.07	10.22 ± 4.99	23	ND	ND	NA	ND	ND	NA	ND	ND	NA
			VTR	ND	ND	NA	0.26	0.36	>379	0.47	0.77	44	ND	ND	NA	0.054	0.07	319	0.26	0.77	>195
	NiV-B	Bangladesh	CPE	11.23 ± 0.63	33.6 ± 1.58	>8.9	0.21 ± 0.063	0.62 ± 0.20	>379	0.41 ± 0.039	1.71 ± 0.66	50									
	HeV	1994	CPE	11.52 ± 1.49	26.11 ± 4.44	>8.7	0.22 ± 0.04	0.65 ± 0.11	>463	0.42 ± 0.023	1.19 ± 0.061	49									
	MV	Rec. $rMV^{EZ}GFP(3)$	REP	4.98 ± 0.37	12.02 ± 2.7	>20	0.063 ± 0.02	0.128 ± 0.016	>1,587	0.082 ± 0.026	0.29 ± 0.043	251									
	hPIV3	Rec. JS-GFP	FFU	4.96 ± 0.05	5.77 ± 0.06	>20	0.063 ± 0.001	0.074 ± 0.002	>1,582	0.091 ± 0.009	0.20 ± 0.008	226									
Pneumoviridae	RSV	Rec. rgRSV0224 (A2)	FFU	4.92 ± 0.47	8.09 ± 0.68	>20	0.088 ± 0.026	0.21 ± 0.033	>,1134	0.12 ± 0.008	0.34 ± 0.047	176									

[a]EBOV, Ebola virus; MARV, Marburg virus; NiV-M, Nipah virus Malaysia strain; NiV-B, Nipah virus Bangladesh strain; HeV, Hendra virus; MV, measles virus; hPIV3, human parainfluenza virus 3; RSV, respiratory syncytial virus.
[b]Rec., recombinant; ZsG, ZsGreen fluorescent protein; GFP, green fluorescent protein.
[c]REP, FFU, CPE, and VTR assays were conducted at 72 hpi. REP, fluorescent reporter; VTR, virus titer reduction; CPE, cytopathic effect; FFU, focus-forming units.
[d]Values were derived from 3 independent experiments performed in biological triplicates. TIME, primary-like human telomerase reverse-transcriptase (hTERT)-immortalized human microvascular endothelial cell line; HSAEC1-KT, hTERT-immortalized small airway epithelial cell line; EC_{50}, EC_{90}, and CC_{50} values were calculated using GraphPad Prism 9 software. EC_{50} and EC_{90}, 50% and 90% effective concentrations; CC_{50}, 50% cytotoxic concentration; SI, selective index (EC_{50}/CC_{50}); ND, not determined; NI, no inhibition; NA, not applicable. The CC_{50} values for each compound in the respective cell lines are indicated in parentheses above the column indicated for SI values.

more active than RVn, it consistently showed 6- to 20-fold less activity than RDV (Fig. 1B to D, middle left and middle right; Table 1; Fig. S2 and S3). Whereas the CC_{50} values for RDV in Huh7 and NCI-H358 cells were 54.2 and 77.2 μM, respectively, ODBG-P-RVn was less cytotoxic in Huh7 cells (CC_{50} = 93.4 μM) and did not show measurable cytotoxicity in NCI-H358 cells even at the highest concentration tested (100 μM) (Fig. 1E, middle right; Table 1).

To further evaluate cell type-specific effects on the antiviral activities of RVn, RDV, and ODBG-P-RVn, we tested them against a smaller subset of reporter viruses in primary-like human telomerase reverse transcriptase (hTERT)-immortalized human microvascular endothelial (TIME) cells (19, 20). In TIME cells, we observed a trend in antiviral activity similar to those in Huh7 and NCI-H358 cells, with ODBG-P-RVn showing 15- to 22-fold greater activity than RVn but 5- to 8-fold less activity than RDV in reporter-based assays (Table 2; Fig. S4A). We further compared the activities of RDV and ODBG-P-RVn by infectious yield assay and observed that both compounds equivalently reduced the infectious yield of EBOV expressing ZsGreen protein (EBOV-ZsG), by up to 4 $\log_{10}$, and that of of NiV-ZsG, by approximately 2 $\log_{10}$, in a dose-dependent manner, with EC_{50} values closely mirroring the values determined in reporter assays (Table 2; Fig. S4B). However, RDV was more cytotoxic (CC_{50} = 17.2 μM) than ODBG-P-RVn ($CC_{50} > 50$ μM), which is reflected in its biphasic inhibition of NiV-ZsG, with cytotoxic inhibition by RDV shown at 16.6 μM (Fig. S4C).

Since ODBG lipid nucleoside modification enhances *in vivo* lung tissue distribution via the chylomicron pathway (21, 22), we compared the activities of the three compounds against filoviruses, paramyxoviruses, and RSV in another primary-like, hTERT-immortalized small airway epithelial cell line (HSAEC1-KT) (23). Notably, the dose-response curves of RDV and ODBG-P-RVn were strikingly similar, with EC_{50} values in the submicromolar range within a 3-fold range of each other; the EC_{50} values for some viruses were almost identical (Fig. 1B to D, right; Table 2; Fig. S5). Furthermore, RDV and ODBG-P-RVn reduced the infectious yields of EBOV-ZsG and NiV-ZsG in HSAEC1-KT cells equivalently, by 5 $\log_{10}$ and 3 $\log_{10}$, respectively, and their EC_{50} values reflected the limited differential in antiviral activities between them (Fig. 1G; Table 2). Although ODBG-P-RVn was more cytotoxic (CC_{50} = 20.5) than RDV ($CC_{50} > 100$) in HSAEC1-KT cells (Fig. 1D, right; Table 2), it also effectively reduced the virus yields at noncytotoxic concentrations. We also evaluated the antiviral activity of the ODBG lipid alone and observed no detectable antiviral activity against any of the viruses tested in HSAEC1-KT cells (data not shown).

Our results demonstrate that ODBG-P-RVn has greater antiviral activity than RVn and has cell type-dependent activity levels that range from moderately lower than to nearly equal to those of RDV. *In vivo*, RDV is converted rapidly to RVn (4–7), which has 0.5 to 2 $\log_{10}$ less activity than RDV against most of the viruses tested. In contrast, ODBG-P-RVn was stable in plasma for >24 h and reached therapeutic plasma levels (above the EC_{90} for SARS-CoV-2) after oral administration of 16.9 mg/kg of body weight to Syrian hamsters; it also did not produce virologically significant levels of RVn (13). Thus, one would predict sustained *in vivo* antiviral activity with ODBG-P-RVn, without substantial generation of RVn, the less active metabolite, in plasma. Taken together, our results support further optimization of ODBG-P-RVn and future *in vivo* evaluation of such monophosphate lipid-modified analogs of RVn for their efficacy against viruses significant to human health.

SUPPLEMENTAL MATERIAL

Supplemental material is available online only.

SUPPLEMENTAL FILE 1, PDF file, 6.8 MB.

ACKNOWLEDGMENTS

We thank Tatyana Klimova for helpful comments in reviewing the manuscript. We thank Pei-Yong Shi (University of Texas Medical Branch) for the kind gift of the SARS-CoV-2 reporter strain expressing mNeonGreen.

The findings and conclusions in this report are those of the authors and do not necessarily represent those of the Centers for Disease Control and Prevention. This work was supported by CDC core funding and by the National Institute of Allergy and Infectious Diseases (grant number RO1-AI131424).

REFERENCES

1. Malin JJ, Suárez I, Priesner V, Fätkenheuer G, Rybniker J. 2020. Remdesivir against COVID-19 and other viral diseases. Clin Microbiol Rev 34:e00162-20. https://doi.org/10.1128/CMR.00162-20.
2. Gilead. 2020. Veklury/remdesivir. FDA approved to treat COVID-19. Gilead, Foster City, CA. https://www.veklury.com/. Accessed 8 July 2021.
3. Beigel JH, Tomashek KM, Dodd LE, Mehta AK, Zingman BS, Kalil AC, Hohmann E, Chu HY, Luetkemeyer A, Kline S, Lopez de Castilla D, Finberg RW, Dierberg K, Tapson V, Hsieh L, Patterson TF, Paredes R, Sweeney DA, Short WR, Touloumi G, Lye DC, Ohmagari N, Oh M-D, Ruiz-Palacios GM, Benfield T, Fätkenheuer G, Kortepeter MG, Atmar RL, Creech CB, Lundgren J, Babiker AG, Pett S, Neaton JD, Burgess TH, Bonnett T, Green M, Makowski M, Osinusi A, Nayak S, Lane HC. 2020. Remdesivir for the treatment of Covid-19—final report. N Engl J Med 383:1813–1826. https://doi.org/10.1056/NEJMoa2007764.
4. Warren TK, Jordan R, Lo MK, Ray AS, Mackman RL, Soloveva V, Siegel D, Perron M, Bannister R, Hui HC, Larson N, Strickley R, Wells J, Stuthman KS, Van Tongeren SA, Garza NL, Donnelly G, Shurtleff AC, Retterer CJ, Gharaibeh D, Zamani R, Kenny T, Eaton BP, Grimes E, Welch LS, Gomba L, Wilhelmsen CL, Nichols DK, Nuss JE, Nagle ER, Kugelman JR, Palacios G, Doerffler E, Neville S, Carra E, Clarke MO, Zhang L, Lew W, Ross B, Wang Q, Chun K, Wolfe L, Babusis D, Park Y, Stray KM, Trancheva I, Feng JY, Barauskas O, Xu Y, Wong P, et al. 2016. Therapeutic efficacy of the small molecule GS-5734 against Ebola virus in rhesus monkeys. Nature 531:381–385. https://doi.org/10.1038/nature17180.
5. Tempestilli M, Caputi P, Avataneo V, Notari S, Forini O, Scorzolini L, Marchioni L, Ascoli Bartoli T, Castilletti C, Lalle E, Capobianchi MR, Nicastri E, D'Avolio A, Ippolito G, Agrati C, COVID 19 INMI Study Group. 2020. Pharmacokinetics of remdesivir and GS-441524 in two critically ill patients who recovered from COVID-19. J Antimicrob Chemother 75:2977–2980. https://doi.org/10.1093/jac/dkaa239.
6. Mackman RL, Hui HC, Perron M, Murakami E, Palmiotti C, Lee G, Stray K, Zhang L, Goyal B, Chun K, Byun D, Siegel D, Simonovich S, Du Pont V, Pitts J, Babusis D, Vijjapurapu A, Lu X, Kim C, Zhao X, Chan J, Ma B, Lye D, Vandersteen A, Wortman S, Barrett KT, Toteva M, Jordan R, Subramanian R, Bilello JP, Cihlar T. 2021. Prodrugs of a 1′-CN-4-aza-7,9-dideazaadenosine C-nucleoside leading to the discovery of remdesivir (GS-5734) as a potent inhibitor of respiratory syncytial virus with efficacy in the African green monkey model of RSV. J Med Chem 64:5001–5017. https://doi.org/10.1021/acs.jmedchem.1c00071.
7. Humeniuk R, Mathias A, Cao H, Osinusi A, Shen G, Chng E, Ling J, Vu A, German P. 2020. Safety, tolerability, and pharmacokinetics of remdesivir, an antiviral for treatment of COVID-19, in healthy subjects. Clin Transl Sci 13:896–906. https://doi.org/10.1111/cts.12840.
8. Shi Y, Shuai L, Wen Z, Wang C, Yan Y, Jiao Z, Guo F, Fu ZF, Chen H, Bu Z, Peng G. 2021. The preclinical inhibitor GS441524 in combination with GC376 efficaciously inhibited the proliferation of SARS-CoV-2 in the mouse respiratory tract. Emerg Microbes Infect 10:481–492. https://doi.org/10.1080/22221751.2021.1899770.
9. Li Y, Cao L, Li G, Cong F, Li Y, Sun J, Luo Y, Chen G, Li G, Wang P, Xing F, Ji Y, Zhao J, Zhang Y, Guo D, Zhang X. 1 February 2021. Remdesivir metabolite GS-441524 effectively inhibits SARS-CoV-2 infection in mouse models. J Med Chem. https://doi.org/10.1021/acs.jmedchem.0c01929.
10. Murphy BG, Perron M, Murakami E, Bauer K, Park Y, Eckstrand C, Liepnieks M, Pedersen NC. 2018. The nucleoside analog GS-441524 strongly inhibits feline infectious peritonitis (FIP) virus in tissue culture and experimental cat infection studies. Vet Microbiol 219:226–233. https://doi.org/10.1016/j.vetmic.2018.04.026.
11. Pedersen NC, Perron M, Bannasch M, Montgomery E, Murakami E, Liepnieks M, Liu H. 2019. Efficacy and safety of the nucleoside analog GS-441524 for treatment of cats with naturally occurring feline infectious peritonitis. J Feline Med Surg 21:271–281. https://doi.org/10.1177/1098612X19825701.
12. Yan VC, Muller F. 2020. Comprehensive summary supporting clinical investigation of GS-441524 for Covid-19 treatment. OSFPREPRINTS. https://doi.org/10.31219/osf.io/mnhxu.
13. Schooley RT, Carlin AF, Beadle JR, Valiaeva N, Zhang X-Q, Clark AE, McMillan RE, Leibel SL, McVicar RN, Xie J, Garretson AF, Smith VI, Murphy J, Hostetler KY. 2021. Rethinking remdesivir: synthesis, antiviral activity and pharmacokinetics of oral lipid prodrugs. Antimicrob Agents Chemother 65:e01155-21. https://doi.org/10.1128/AAC.01155-21.
14. Xie X, Muruato A, Lokugamage KG, Narayanan K, Zhang X, Zou J, Liu J, Schindewolf C, Bopp NE, Aguilar PV, Plante KS, Weaver SC, Makino S, LeDuc JW, Menachery VD, Shi PY. 2020. An infectious cDNA clone of SARS-CoV-2. Cell Host Microbe 27:841–848.e3. https://doi.org/10.1016/j.chom.2020.04.004.
15. Lo MK, Jordan R, Arvey A, Sudhamsu J, Shrivastava-Ranjan P, Hotard AL, Flint M, McMullan LK, Siegel D, Clarke MO, Mackman RL, Hui HC, Perron M, Ray AS, Cihlar T, Nichol ST, Spiropoulou CF. 2017. GS-5734 and its parent nucleoside analog inhibit Filo-, Pneumo-, and Paramyxoviruses. Sci Rep 7:43395. https://doi.org/10.1038/srep43395.
16. Lo MK, Spengler JR, Krumpe LRH, Welch SR, Chattopadhyay A, Harmon JR, Coleman-McCray JD, Scholte FEM, Hotard AL, Fuqua JL, Rose JK, Nichol ST, Palmer KE, O'Keefe BR, Spiropoulou CF. 2020. Griffithsin inhibits Nipah virus entry and fusion and can protect Syrian golden hamsters from lethal Nipah virus challenge. J Infect Dis 221:S480–S492. https://doi.org/10.1093/infdis/jiz630.
17. Lo MK, Jordan PC, Stevens S, Tam Y, Deval J, Nichol ST, Spiropoulou CF. 2018. Susceptibility of paramyxoviruses and filoviruses to inhibition by 2′-monofluoro- and 2′-difluoro-4′-azidocytidine analogs. Antiviral Res 153:101–113. https://doi.org/10.1016/j.antiviral.2018.03.009.
18. Welch SR, Chakrabarti AK, Wiggleton Guerrero L, Jenks HM, Lo MK, Nichol ST, Spiropoulou CF, Albariño CG. 2018. Development of a reverse genetics system for Sosuga virus allows rapid screening of antiviral compounds. PLoS Negl Trop Dis 12:e0006326. https://doi.org/10.1371/journal.pntd.0006326.
19. Siegel D, Hui HC, Doerffler E, Clarke MO, Chun K, Zhang L, Neville S, Carra E, Lew W, Ross B, Wang Q, Wolfe L, Jordan R, Soloveva V, Knox J, Perry J, Perron M, Stray KM, Barauskas O, Feng JY, Xu Y, Lee G, Rheingold AL, Ray AS, Bannister R, Strickley R, Swaminathan S, Lee WA, Bavari S, Cihlar T, Lo MK, Warren TK, Mackman RL. 2017. Discovery and synthesis of a phosphoramidate prodrug of a pyrrolo[2,1-f][triazin-4-amino] adenine C-nucleoside (GS-5734) for the treatment of Ebola and emerging viruses. J Med Chem 60:1648–1661. https://doi.org/10.1021/acs.jmedchem.6b01594.
20. Venetsanakos E, Mirza A, Fanton C, Romanov SR, Tlsty T, McMahon M. 2002. Induction of tubulogenesis in telomerase-immortalized human microvascular endothelial cells by glioblastoma cells. Exp Cell Res 273:21–33. https://doi.org/10.1006/excr.2001.5424.
21. Hostetler KY, Beadle JR, Trahan J, Aldern KA, Owens G, Schriewer J, Melman L, Buller RM. 2007. Oral 1-O-octadecyl-2-O-benzyl-sn-glycero-3-cidofovir targets the lung and is effective against a lethal respiratory challenge with ectromelia virus in mice. Antiviral Res 73:212–218. https://doi.org/10.1016/j.antiviral.2006.10.009.
22. Hostetler KY. 2009. Alkoxyalkyl prodrugs of acyclic nucleoside phosphonates enhance oral antiviral activity and reduce toxicity: current state of the art. Antiviral Res 82:A84–A98. https://doi.org/10.1016/j.antiviral.2009.01.005.
23. Ramirez RD, Sheridan S, Girard L, Sato M, Kim Y, Pollack J, Peyton M, Zou Y, Kurie JM, Dimaio JM, Milchgrub S, Smith AL, Souza RF, Gilbey L, Zhang X, Gandia K, Vaughan MB, Wright WE, Gazdar AF, Shay JW, Minna JD. 2004. Immortalization of human bronchial epithelial cells in the absence of viral oncoproteins. Cancer Res 64:9027–9034. https://doi.org/10.1158/0008-5472.CAN-04-3703.